# Microscopic description of nuclear structure around $^{80}$Zr

Wen-hua Zou,[1,2,*] Yuan Tian,[1] Jian-zhong Gu,[1,3,†] Shui-fa Shen,[2] Jiang-ming Yao,[4] Bang-bao Peng,[1] and Zhong-yu Ma[1,3]
[1]*China Institute of Atomic Energy, P.O. Box 275 (18), Beijing 102413, China*
[2]*School of Nuclear Engineering and Technology, East China Institute of Technology, Fuzhou, Jiangxi 344000, China*
[3]*Center of Theoretical Nuclear Physics, National Laboratory of Heavy Ion Accelerator of Lanzhou, Lanzhou 730000, China*
[4]*School of Physical Science and Technology, Southwest University, Chongqing 400715, China*
(Received 27 December 2009; revised manuscript received 4 April 2010; published 10 August 2010)

A new approach for the calculation of angular momentum projected potential energy surfaces (AMPPESs) is proposed which combines the projected shell model with a quadrupole constrained relativistic Hartree-Bogoliubov (RHB) theory in which the NL3 effective interaction is chosen for the relativistic mean-field effective Lagrangian and a separable Gogny D1S interaction for the pairing force (QCRHB-NL3 + separable Gogny D1S force theory). We apply this approach to compute the AMPPESs of $^{80,82,84}$Zr nuclei up to high spins and investigate the spin-induced shape transitions and decay out of the superdeformed (SD) bands in these nuclei. We find that the shape transitions occur in $^{80}$Zr and $^{84}$Zr, which are driven by the rotational alignments of the nucleons in the $1g_{9/2}$ orbitals, and a strong shape mixing happens in $^{82}$Zr. Moreover, it is shown that the barrier separating the SD states and normal deformed (or spherical) states becomes lower and narrower for $^{82}$Zr and $^{84}$Zr at high spins, indicating that the decay out of the SD bands could occur at high spins. For $^{80}$Zr, however, there is no decay out of the SD band because the barrier is so high and thick. Meanwhile, the QCRHB-NL3 + separable Gogny D1S force theory is employed to calculate the ground-state potential energy surfaces and the single-particle levels of these nuclei, which in turn are used to determine and analyze the equilibrium shapes and discuss the shape coexistence of these nuclei. In addition, this theory is compared with other state-of-the-art mean-field theories to justify its use to study the ground-state potential energy surfaces of $^{80,82,84}$Zr.

DOI: 10.1103/PhysRevC.82.024309 PACS number(s): 21.10.Pc, 21.10.Re, 21.60.Cs, 27.50.+e

## I. INTRODUCTION

One of the great challenges of modern nuclear structure physics is understanding microscopically the evolution of structure, in particular, the development of deformation, shape coexistence, and shape transition. This effort has expanded tremendously in recent years with the advent of new generations of facilities for the production and study of exotic nuclei. The shape of an atomic nucleus is one of the most important nuclear bulk properties, and shape coexistence is understood as the occurrence of two (or more) nearly equally deep minima in the potential energy surface at different deformations. As a result of the low density of single-particle energy levels, the nuclear shapes are strongly configuration dependent. They are predicted to vary not only with particle number but also with excitation energy and spin.

Proton-rich nuclei near the $N = Z$ line in the mass region $A \approx 80$ is known to provide abundant and exotic nuclear structure phenomena, which are often characterized by shape coexistence. This stems from the fact that large parts of protons and neutrons of these nuclei are distributed in the $pfg$ orbitals; thus, their level density is high and there is a severe competition between single-particle motion and collective motion. Moreover, the intruder of the $1g_{9/2}$ orbitals, which are located just above the $N = 40$ subclosure, further complicates the structure and plays an important role in the shape coexistence. These nuclei, therefore, offer an ideal place to study the evolution of nuclear structure with particle number, excitation energy, and spin.

Experimental evidence of the shape coexistence of these nuclei has been found, for instance, for Se and Kr isotopes [1–5]. Meanwhile, since the first observation of a superdeformed (SD) band ($\beta_2 \approx 0.55$) in the nuclei with $N, Z \approx 40$ [6], it has been a focal issue to investigate the SD bands in nuclei of mass $A \approx 80$ [7–9]. We would mention that in Ref. [9] the linking transitions between the yrast SD states and normal deformed (ND) states were observed in the nucleus of $^{84}$Zr. This is the first observation of such transitions in the mass region $A \approx 80$.

There have also been many theoretical studies on the structure of these nuclei. For the shape coexistence, the first studies were performed for $^{72}$Kr and a few neighboring nuclei with the help of the Nilsson-Strutinsky approach [10]. Detailed calculations have been carried out since then with an improved microscopic-macroscopic model [11], with self-consistent mean-field models using nonrelativistic Skyrme [12] and Gogny [13] interactions, as well as with relativistic Lagrangians [14–16] and with the angular momentum and particle-number projected generator coordinate method [17]. These studies confirm the presence of oblate and prolate minima in the potential energy surface of some lighter Kr, Sr, and Zr isotopes. Sometimes, however, their predictions are not consistent with each other. For instance, Ref. [17] predicted that the ground state of the nucleus of $^{80}$Zr is spherical; nevertheless, it is predicted to be prolate in Ref. [15]. Oblate ground states were predicted for the nuclei of $^{82}$Zr and $^{84}$Zr in Ref. [15], but they became prolate based on the total Routhian surfaces calculation in Refs. [18,19].

*zouwenhua840709@163.com
†gujianzhong2000@yahoo.com.cn

 

The nucleus of $^{80}$Zr is indeed one of the typically exotic nuclei in the $A \approx 80$ mass region, which has the unique structural feature that both the proton number and the neutron number are semimagic. Its neighboring nuclei, $^{82,84}$Zr, are expected to have quite different nuclear structures from that of $^{80}$Zr because more neutrons occupy the $1g_{9/2}$ orbitals. All of the above conditions constitute a challenge for a theoretical description of the nuclear structures of $^{80,82,84}$Zr nuclei and might be the reasons why the above-mentioned theoretical predictions are sometimes inconsistent with each other. Therefore, further studies are needed to obtain a more precise nuclear structure of $^{80,82,84}$Zr nuclei.

The physics of exotic nuclei necessitates a unified and self-consistent treatment of mean-field and pairing correlations, which is crucial for an accurate description of the ground states of exotic nuclei. This has actually led to the formulation and development of the relativistic Hartree-Bogoliubov (RHB) theory [20], which was successfully employed in the study of the ground states of exotic nuclei. In the present article, we investigate the nuclear structures of the three zirconium isotopes $^{80,82,84}$Zr. Their shapes and shape coexistence are studied, for the first time, based on the quadrupole constrained RHB theory, in which the relativistic mean-field (RMF) Lagrangian is described by the NL3 effective interaction [21] and the pairing correlations by a separable Gogny D1S force [22]. For convenience, we denote the RHB theory as QCRHB-NL3 + separable Gogny D1S force theory. The parameters involved in this separable force are adjusted to reproduce the pairing properties of the Gogny D1S force [23] in nuclear matter. It preserves translational invariance and has finite range. Applying the well-known techniques of Talmi and Moshinsky [24–26], it was shown in Ref. [22] that this separable force can be represented by a sum of separable terms that converges quickly. This avoids the complicated problem of a cutoff at large momenta or energies inherent in zero-range pairing forces. And this separable force has a behavior very similar to the Gogny D1S force. To examine the change of the nuclear structures with the spin (the angular momentum of a nucleus), we calculate the potential energy surfaces with given angular momenta by combining the QCRHB-NL3 + separable Gogny D1S force theory and the angular momentum projected shell model (PSM) [27]. The potential energy surfaces actually allow us to study the shape transitions and decay out properties of the SD bands of these nuclei. Note that all the calculations in the present article assume an axial symmetry.

The article is arranged as follows. In Sec. II, the PSM, QCRHB-NL3 + separable Gogny D1S force theory, and method to calculate the angular momentum projected potential energy surfaces (AMPPESs) are introduced. Results and discussion are given in Sec. III. Single-particle levels (SPLs) calculated with the QCRHB-NL3 + separable Gogny D1S force theory are used to analyze the stability of the equilibrium shapes of $^{80,82,84}$Zr nuclei and their shape coexistence. Their shape transitions and decay out of their SD bands is discussed based on the AMPPESs obtained by combining the QCRHB-NL3 + separable Gogny D1S force theory with the PSM. In addition, the results for the equilibrium shapes, shape coexistence, shape transitions, and decay out of the SD bands that are obtained by other theoretical methods are presented for comparison. Finally, we give a summary in Sec. IV.

## II. THEORETICAL FRAMEWORK

### A. Angular momentum projected shell model

During the past decades, the angular momentum projected shell model [27–29] has become a standard tool to study the nuclear rotational properties up to high spins. The PSM is a spherical shell model truncated in a deformed basis and solves the many-nucleon system fully quantum mechanically. The PSM proceeds as follows. Starting from the Nilsson + BCS procedure, the shell model truncation is first performed in the multi-quasiparticle (multi-qp) basis by selecting low-lying states; then the rotational symmetry (and the number conservation, if necessary) is restored for these (multi-qp) states by the projection method to form a spherical (many-body) basis in the laboratory frame; finally, the Hamiltonian is diagonalized in this basis.

The detailed description of the PSM calculations for the proton-rich nuclei in the mass region $A \approx 80$ can be found in Ref. [29]. Therefore, we only recapitulate the most relevant points of the PSM that are used in the calculations for $^{80,82,84}$Zr nuclei. For each nucleon, first we diagonalize the Nilsson Hamiltonian for the known quadrupole and hexadecapole deformation parameters [30], then we carry out the usual BCS procedure to take the monopole pairing force into account. This defines the Nilsson + BCS quasiparticle basis. Three major shells ($N = 2, 3, 4$) for both neutrons and protons are used, and the shell model space includes the zero-, two-, and four-quasiparticle (qp) states:

$$|\phi_k\rangle = \{|0\rangle, a^+_{n_i}a^+_{n_j}|0\rangle, a^+_{p_i}a^+_{p_j}|0\rangle, a^+_{n_i}a^+_{n_j}a^+_{p_i}a^+_{p_j}|0\rangle\}, \quad (1)$$

where $a^+$ is the creation operator for a qp, and the index $n$ ($p$) denotes the neutron (proton) Nilsson quantum numbers which run over the low-lying orbitals below the cutoff energy. The corresponding qp vacuum is $|0\rangle$. The indices $n$ and $p$ in Eq. (1) are general; for example, a 2qp state can be of positive (or negative) parity if both quasiparticles $i$ and $j$ are from the same (or two neighboring) major shell(s). Positive and negative parity states span the entire configuration space with the corresponding matrix in a block-diagonal form classified by parity. It is important to note that for the $N = Z$ nuclei under consideration, unperturbed 2qp states of $a^+_{n_i}a^+_{n_j}|0\rangle$ and $a^+_{p_i}a^+_{p_j}|0\rangle$ with the same configuration can occur pairwise as nearly degenerate states.

In our calculations, the PSM uses the pairing forces plus a quadrupole-quadrupole correlation Hamiltonian [27] (that has been known to be essential in nuclear structure calculations [12]) with inclusion of the quadrupole-pairing term

$$\hat{H} = \hat{H}_0 - \frac{\chi}{2}\sum_\mu \hat{Q}^+_\mu \hat{Q}_\mu - G_M \hat{P}^+\hat{P} - G_Q \sum_\mu \hat{P}^+_\mu \hat{P}_\mu. \quad (2)$$

The first term, $\hat{H}_0$, is the spherical harmonic oscillator single-particle Hamiltonian. Note that, in the Hartree-Fock-Bogoliubov single-particle Hamiltonian resulting from the

above many-body Hamiltonian, the contribution from the quadrupole-quadrupole correlation can be identified as the Nilsson potential. As a result, the strength of the quadrupole-quadrupole correlation $\chi$ can be determined in such a way that it has a self-consistent relation with the quadrupole deformation $\varepsilon_2$. (For more details, see formulas (2.45) and (2.51) of Ref. [27].) The monopole pairing force constant $G_M$ is determined by the BCS gap equation, which is explained below.

In the BCS calculation, as usual, we only take the monopole pairing force into account and use the following four-point formulas to evaluate the pairing gap parameters $\Delta_p$ and $\Delta_n$ [31]:

$$\Delta_p = \frac{1}{4}[B(N, Z-2) - 3B(N, Z-1) + 3B(N, Z) - B(N, Z+1)], \quad (3)$$

$$\Delta_n = \frac{1}{4}[B(N-2, Z) - 3B(N-1, Z) + 3B(N, Z) - B(N+1, Z)], \quad (4)$$

for which the values of the total nuclear binding energy $B$ are taken from Ref. [32]. The results for the three nuclei are given in Table I. The values of the hexadecapole deformation parameter $\varepsilon_4$ taken from the compilation of Möller *et al.* [33] are also presented in Table I. The spin-orbit force parameters appearing in the Nilsson potential, $\kappa$ and $\mu$, are taken from Ref. [34] and are a modified version of that in Ref. [35] and were fitted to the latest experimental data for proton-rich nuclei with proton or neutron numbers $28 \leqslant N \leqslant 40$. With the above-mentioned pairing gap parameters, we solve the BCS equations. In turn, we use the solutions to determine the monopole pairing force constant by means of the gap equation. As to the strength parameter $G_Q$ for the quadrupole pairing, it is simply assumed to be $G_Q = \gamma G_M$ as commonly used in the PSM calculations [27]. The proportionality constant $\gamma$ is fixed to be 0.16 in the present calculations.

The eigenvalue equation of the PSM for a given spin $I$ takes the form

$$\sum_{k'} \{H^I_{kk'} - E^I N^I_{kk'}\} F^I_{k'} = 0, \quad (5)$$

where the Hamiltonian and norm matrix elements are respectively defined by

$$H^I_{kk'} = \langle \phi_k | \hat{H} \hat{P}^I_{KK'} | \phi_{k'} \rangle, \quad N^I_{kk'} = \langle \phi_k | \hat{P}^I_{KK'} | \phi_{k'} \rangle, \quad (6)$$

where $\hat{P}^I_{MK}$ is the angular momentum projection operator [27]. The expectation values of the Hamiltonian with respect to a "rotational band $k$" $H^I_{kk}/N^I_{kk}$ are the so-called band energies.

We use a computer code [36] to perform the PSM calculations in this article. And the configuration space is constructed for these nuclei by selecting the qp states close to the Fermi energy in the $N = 4$ major shell for both neutrons and protons and forming multi-qp states from them. The dimension of the qp basis is around 100 and all the calculations are for the positive-parity states.

TABLE I. Relevant parameters used in the projected shell model.

| Nuclei | $\Delta_p$ (MeV) | $\Delta_n$ (MeV) | $\gamma$ | $\varepsilon_4$ |
|---|---|---|---|---|
| $^{80}$Zr | 1.7935 | 1.9225 | 0.16 | 0.087 |
| $^{82}$Zr | 1.4645 | 1.5400 | 0.16 | 0.000 |
| $^{84}$Zr | 1.5845 | 1.5325 | 0.16 | 0.000 |

### B. The QCRHB-NL3 + separable Gogny D1S force theory

Let us start with the relativistic Hartree-Bogoliubov theory, a theory developed decades ago by Ring and his collaborators [37,38]. In the Hartree approximation for a consistent mean field, the RHB equations read

$$\begin{pmatrix} \hat{h}_D - \lambda & \hat{\Delta} \\ -\hat{\Delta}^* & -\hat{h}_D + \lambda \end{pmatrix} \begin{pmatrix} U_k(\mathbf{r}) \\ V_k(\mathbf{r}) \end{pmatrix} = E_k \begin{pmatrix} U_k(\mathbf{r}) \\ V_k(\mathbf{r}) \end{pmatrix}, \quad (7)$$

where $\hat{h}_D$ is the single-nucleon Dirac Hamiltonian,

$$\hat{h}_D = -i\boldsymbol{\alpha} \cdot \nabla + \beta[m + g_\sigma \sigma(\mathbf{r})] + g_\omega \tau_3 \omega^0(\mathbf{r}) + g_\rho \rho^0(\mathbf{r}) + e\frac{(1-\tau_3)}{2} A^0(\mathbf{r}) - m. \quad (8)$$

The Dirac Hamiltonian contains the mean-field potentials of the isoscalar scalar $\sigma$ meson, the isoscalar vector $\omega$ meson, the isovector vector $\rho$ meson, as well as the photon; $m$ is the nucleon mass, and the term $-m$ subtracts the rest mass and normalizes the energy scale to the continuum limit. The chemical potential is to be determined by the subsidiary particle number condition, where the expectation value of the particle number operator in the ground state equals the number of nucleons. The column vectors are the quasiparticle spinors, and $E_k$ are the quasiparticle energies; $\hat{\Delta}$ denotes the pairing fields, which is an integral operator with the kernel

$$\Delta_{ab}(\mathbf{r}, \mathbf{r}') = \frac{1}{2} \sum_{c,d} V_{abcd}(\mathbf{r}, \mathbf{r}') \kappa_{cd}(\mathbf{r}, \mathbf{r}'), \quad (9)$$

where $a, b, c, d$ denote the quantum numbers that specify the Dirac indices of the spinor. They run over the two spin orientations and the large and small components. $V_{abcd}(\mathbf{r}, \mathbf{r}')$ are matrix elements of the two-body pairing interaction. The pairing tensor is defined as

$$\kappa_{cd}(\mathbf{r}, \mathbf{r}') = \sum_{E_k > 0} U_{ck}(\mathbf{r})^* V_{dk}(\mathbf{r}'). \quad (10)$$

The RHB theory with Gogny pairing provides an excellent tool for the description of ground-state properties of nuclei such as deformation and shape coexistence [20,39–41]. Nevertheless, its applications are limited because of its numerical complexity.

A few years ago, Duguet proposed a method to derive a separable form of the pairing interaction by recasting the gap equation, written in terms of the bare force, into a fully equivalent pairing problem [42]. This separable pairing force can reproduce the pairing properties provided by the realistic Argonne v18 (AV18) force very accurately. Although this separable force is finite ranged, nonlocal, total-momentum dependent, and density dependent, it has a very simple form and makes mean-field plus Bogoliubov calculations in the coordinate space tractable.

Recently Tian *et al.* introduced a new separable form of the pairing force for the RHB calculations in spherical nuclei [22,43]. The parameters of this separable force are adjusted to reproduce the pairing properties of the Gogny force in nuclear matter. The gap equation in the $^1S_0$ channel has the form

$$\Delta(k) = -\int_0^\infty \frac{k'^2 dk'}{2\pi^2}\langle k|V^{^1S_0}|k'\rangle \frac{\Delta(k')}{2E(k')}, \tag{11}$$

where a separable form of the pairing force is introduced [22],

$$\langle k|V_{\rm sep}^{^1S_0}|k'\rangle = -Gp(k)p(k'). \tag{12}$$

A simple Gaussian ansatz $p(k) = e^{-a^2k^2}$ is assumed. In Ref. [22], the two parameters $G$ and $a$ were fitted to the density dependence of the gap at the Fermi surface $\Delta(k_F)$ as given by the finite-range Gogny force. Comparing with the Gogny force, we found two sets of parameters $G = 738$ MeV fm$^3$ and $a = 0.636$ fm for the parameter set D1 [44] and $G = 728$ MeV fm$^3$ and $a = 0.644$ fm for the set D1S [45].

This pairing force is separable in momentum space. In coordinate space the translational invariance leads to a $\delta$ force in the center-of-mass coordinates and therefore, at first glance, translational invariance forbids exact separability. However, using the well-known techniques of Talmi and Moshinsky [24–26], it was shown that this force can be represented by a sum of separable terms that converges rapidly [22]. This simple separable force can reproduce the pairing properties of the ground states for spherical nuclei on almost the same footing as the original Gogny pairing interaction. Furthermore, Tian *et al.* applied this separability technique of pairing force to the axially deformed RHB calculations [46]. For axially symmetric shapes, the densities are invariant with respect to a rotation around the symmetry axis. Therefore, it is convenient to work in cylindrical coordinates. Because Talmi and Moshinsky's techniques are restricted to spherical coordinates, Tian *et al.* developed similar techniques for cylindrical coordinates working in an anisotropic oscillator basis. Again the matrix elements of the pairing force in this basis are no longer fully separable. Nevertheless, they can be expanded, as in the spherical case, into a series of separable terms. Obviously the convergence of this expansion is not as fast as in the spherical case, but it is still quick enough to save considerable numerical effort compared to the full Gogny calculations.

Using the pairing force separability technique for axially deformed nuclei, we compute the total binding energy of $^{80,82,84}$Zr nuclei as a function of the quadrupole deformation in the framework of the QCRHB-NL3 + separable Gogny D1S force theory. The computer code used for this purpose was developed by one of the authors of this article (Y. Tian) using the framework of the computer program for the relativistic mean-field description of the ground-state properties of even-even axially deformed nuclei [47]. Note that the constrained RHB equations are solved by expanding the Dirac spinors in an axially deformed oscillator basis with 16 major oscillator shells, and the convergence of this expansion has been checked.

### C. Angular momentum projected potential energy surfaces

Let us now briefly introduce the method of calculation of the AMPPESs. The Hamiltonian of the PSM does not contain the Coulomb interaction of protons [27,29,36], which is indispensable for the potential energy surface (PES). To remedy this shortcoming of the PSM and compute the AMPPESs, we combine the PSM with the QCRHB-NL3 + separable Gogny D1S force theory, both of which were introduced in Sec. II B. We first calculate the ground-state PES based on the QCRHB-NL3 + separable Gogny D1S force theory. Then we calculate the PES with a given angular momentum in the framework of the PSM. Finally, the energy difference between the PSM-calculated PES with a nonzero angular momentum and that with zero spin is added to the ground-state PES, and a new PES is then formed, which, roughly speaking, has a given angular momentum. Certainly, since angular momentum projection has not yet been performed for the ground-state PES, anything added to the top of it is also unprojected. Those new PESs together with the ground-state PES constitute a group of PESs with (approximate) given angular momenta. We would say that the ground-state PES serves as a kind of bandhead of the PES group.

We give some further justifications for our combined method of calculating the AMPPESs as follows.

(a) For a great variety of many-body systems (including the nucleus), it is possible to describe the excitation spectra in terms of elementary modes of excitation representing the different, approximately independent, fluctuations about equilibrium [48]. This implies a separation of scale between the excitations of many-body systems and their ground-state energies and therefore justifies our combined method where nuclear ground states are treated with the RHB, and nuclear excitations are described by the PSM.

(b) The Nilsson + BCS quasiparticle states in the PSM are different from the RHB quasiparticle states, which is also justified by the separation of scale. In fact, the former only serves as a basis for the PSM.

(c) The Hamiltonian used in the PSM [see Eq. (2)] is rather schematic for nuclear excitations; however, it takes into account the most important long-range correlations (the quadrupole-quadrupole correlation) and the most important short-range correlations (the pairing forces) [49]. In this sense, the PSM is a shell-model-like approach.

## III. RESULTS AND DISCUSSION

In this section we present and discuss the results of the equilibrium shapes, shape coexistence, shape transitions, and decay out of the SD bands for $^{80,82,84}$Zr nuclei. In Sec. III A, the ground-state PESs and SPLs for these nuclei based on the QCRHB-NL3 + separable Gogny D1S force theory are presented. A comparison of the QCRHB-NL3 + separable Gogny D1S force theory with other state-of-the-art mean-field theories is made to justify the use of this theory to study the ground-state properties of these nuclei in Sec. III B. The shape coexistence of these nuclei is described, analyzed, and compared with that given by other state-of-the-art mean-field theories in Sec. III C. In Sec. III D, the AMPPESs calculated

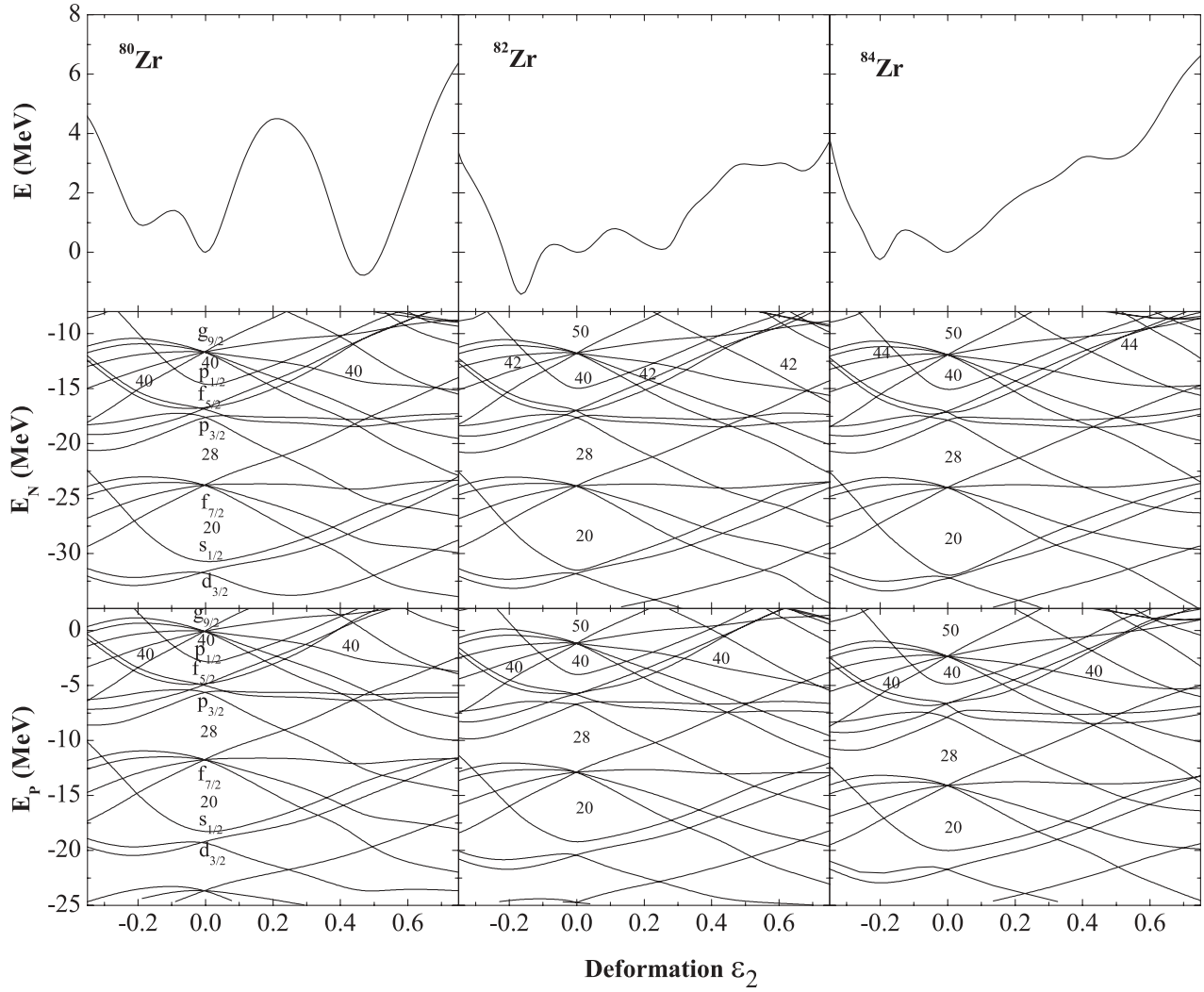


FIG. 1. Ground-state total binding energies (ground-state potential energy surfaces) calculated with the QCRHB-NL3 + separable Gogny D1S force theory as functions of the quadrupole deformation $\varepsilon_2$ compared with the single-neutron levels ($E_N$) and the single-proton levels ($E_P$) for $^{80,82,84}$Zr nuclei. The zero energy is set to be the total energy at $\varepsilon_2 = 0$. The numbers denote the nucleon numbers at pronounced or important shell gaps.

based on the projected shell model together with the QCRHB-NL3 + separable Gogny D1S force theory are described. We alternatively calculate the AMPPESs for these nuclei by replacing the QCRHB-NL3 + separable Gogny D1S force theory by a relativistic point-coupling model for comparison. The two kinds of AMPPESs are used to discuss the shape transitions, strong shape mixing, and decay out of the SD bands for these nuclei.

### A. Single-particle levels and ground-state potential energy surfaces

Deformation plays a key role in the structure of $N = Z$ nuclei. Because of the coinciding low-level densities in both the proton and neutron nuclear potentials, the nuclear shapes are extremely configuration dependent. The SPLs give important information for interpreting nuclear stable deformations. With the Dirac spinors obtained by solving the constrained RHB equations, one can construct the single-particle density matrix and determine the SPLs in the canonical basis [20]. Based on the QCRHB-NL3 + separable Gogny D1S force theory, we calculated the single-neutron levels and single-proton levels together with the ground-state total binding energies (namely, the ground-state potential energy surfaces) as functions of quadrupole deformation $\varepsilon_2$ as exhibited in Fig. 1. From the SPL diagrams and the ground-state PESs, one can find that the minima of the potential energy surfaces correspond to the shell gaps of the SPL diagrams. For example, the three minima of $^{80}$Zr are located at $\varepsilon_2 = -0.2$, 0.0, and 0.475, respectively, and they correspond to the three large shell gaps in the SPL diagram, which stabilize the nucleus. Similar situations can be found for $^{82,84}$Zr nuclei. Since $Z = 40$ is a subclosed shell and has a semimagic character, a spherical shape exists in each of the three zirconium isotopes (see Fig. 1). The ground-state PESs allow us to determine the equilibrium shapes (the lowest minimum). We find that $\varepsilon_2 = +0.475$ for $^{80}$Zr, $\varepsilon_2 = -0.175$

for $^{82}$Zr, and $\varepsilon_2 = -0.200$ for $^{84}$Zr. These values are consistent with the experimental data: a strongly prolate shape $\beta_2 > +0.4$ for $^{80}$Zr [50], $|\beta_2| \approx 0.3$ for $^{82}$Zr [18], and $|\beta_2| \approx 0.2$ for $^{84}$Zr [19]. There is a link between the two quadrupole deformation parameters $\varepsilon_2$ and $\beta_2$, $\beta_2 \approx 0.95\varepsilon_2$ [49].

### B. Comparison of the QCRHB-NL3 + separable Gogny D1S force theory with other state-of-the-art mean-field theories

To justify the use of the QCRHB-NL3 + separable Gogny D1S force theory to study the ground-state properties of the three nuclei, we make a comparison of this theory with other state-of-the-art mean-field theories: the Hartree-Fock-Bogoliubov (HFB) theory with D1S Gogny interaction and the relativistic mean-field theories with point-coupling force. Let us start with an overview of these theories.

In the nonrelativistic framework, thanks to the high computer power available nowadays, large-scale HFB axial mean-field calculations based on the D1S Gogny interaction (HFB full Gogny D1S) were recently fulfilled for nearly 7000 nuclei from proton to neutron drip lines by a French group [51]. The ground-state total binding energies (or PESs) as functions of the quadrupole deformation for these nuclei were determined [52]. In the calculation of the PESs using the quadrupole constrained HFB full Gogny D1S approach, however, angular momentum projection was not performed.

Indeed, angular momentum projection, which separates the contribution from different angular momenta to the mean-field states and generates wave functions in the laboratory frame with good angular momenta, has been a goal of nuclear physicists for many years. However, because of its numerical complexity, only in the past decade was it possible to apply such projection procedures in the context of nonrelativistic self-consistent mean-field theory, with realistic Skyrme force [53–56] and the Gogny force [57,58].

In the relativistic framework, angular momentum projection has so far been restricted to the mean-field level with the relativistic point-coupling force [59–61]. In practical application of the relativistic mean-field point-coupling theory, the most frequently used nonlinear coupling parameter sets are PC-LA [62] and PC-F1 [63]. PC-LA is determined by the ground-state observables for $^{16}$O, $^{88}$Sr and $^{208}$Pb. Because of the explicit omission of the pairing interaction, the pairing effects are not included in the fitting procedure. Moreover, the test for naturalness in Ref. [64] shows that only six of the nine coupling constants are natural. As an improvement, PC-F1 is optimized to the observables of 17 spherical nuclei, including some open-shell nuclei, and the pairing correlation is considered through a standard BCS approach in the fitting procedure. Furthermore, all the coupling constants of PC-F1 turn out to be natural [63]. Nevertheless, the predicted isospin dependence of binding energy by PC-F1 along either the isotopic or the isotonic chains deviates from the data remarkably.

Very recently, Zhao *et al.* proposed a new parametrization named PC-PK1 [65]. They fitted to the observables for 60 selected spherical nuclei, including the binding energies, charge radii, and empirical pairing gaps. All nine parameters in PC-PK1 proved to be natural in the test for naturalness. It was found that PC-PK1 can achieve not only the same quality in the description for the charge radius as other popular effective interactions but also higher accuracy for the binding energy. Moreover, PC-PK1 improves the description for isospin dependence of binding energy along either the isotopic or isotonic chains, which makes its application to exotic nuclei more reliable.

We calculated the angular momentum projected ground-state total binding energies (PESs) for $^{80,82,84}$Zr nuclei within the quadrupole constrained relativistic mean-field framework with the PC-PK1 parameter set. The pairing correlation is considered through a standard BCS method with a density-independent $\delta$ pairing force [61]. We denote this approach by AMP-QCPC-PK1+BCS. The ground-state PESs calculated with the AMP-QCPC-PK1+BCS approach are displayed in Fig. 2 with those given by the QCHFB full Gogny D1S approach [52] and by the QCRHB-NL3 + separable Gogny D1S force theory. From Fig. 2, one can see that the AMP-QCPC-PK1+BCS approach yields equilibrium shapes that are consistent with the experimental data. However, the QCHFB full Gogny D1S approach predicts spherical equilibrium

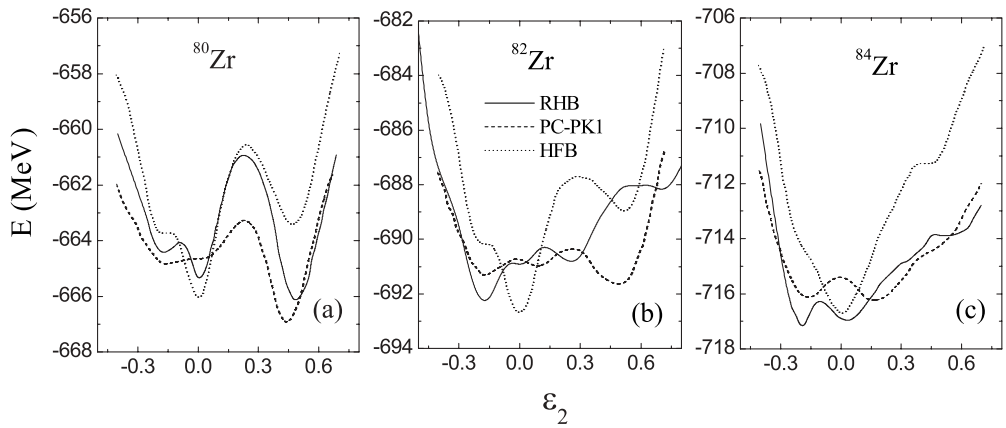


FIG. 2. Ground-state total binding energies (PESs) calculated with different approaches for various spins as functions of deformation variable $\varepsilon_2$ for nuclei of $^{80}$Zr, $^{82}$Zr, and $^{84}$Zr. The solid lines are given by QCRHB-NL3 + separable Gogny D1S force theory, the dashed lines by the AMP-QCPC-PK1+BCS approach, and the dotted lines by the QCHFB full Gogny D1S approach.

shapes for the three nuclei, which are inconsistent with the experimental data. So this approach is not so suited to study the ground-state PESs of the three nuclei, although it is a very coherent approach based on a good phenomenological effective interaction that captures most of the physics of nuclei and works beautifully for many other nuclei.

Both the AMP-QCPC-PK1+BCS approach and the QCRHB-NL3 + separable Gogny D1S force theory yield equilibrium shapes that are consistent with the experimental data; therefore, the ground-state PESs given by the two relativistic theories are used as the bandheads of the groups of the PESs with given angular momenta (or approximate given angular momenta) in Sec. III D. Nevertheless, the values of the equilibrium shapes given by the two relativistic approaches are quite different from each other, especially for $^{82,84}$Zr nuclei. Moreover, we mention here that the QCRHB-NL3 + separable Gogny D1S force theory actually has some advantages over the AMP-QCPC-PK1+BCS approach: Its mean field is meson exchange based, and nucleon-nucleon interaction is of finite range and has clear physical origin; therefore, its mean field is much more realistic than that of the AMP-QCPC-PK1+BCS approach, in which the nucleon-nucleon interaction is a contact force. Its pairing force is of finite range and coupled with a proper Bogoliubov transformation, which is more realistic than the $\delta$ force at the BCS level used in the AMP-QCPC-PK1+BCS approach.

In fact, the RMF with the NL3 effective interaction is able to describe many ground-state properties of finite nuclei all over the periodic table. For instance, an RMF-NL3 + BCS approach [66] predicted the equilibrium shapes for $^{80,82,84}$Zr nuclei, which are also consistent with the experimental data. And the RHB-NL3+Gogny-D1S-force proved a very successful tool for the description of various properties of ground states as well as of excited states with collective character [67]. In addition, for deformed $^{80,82,84}$Zr nuclei, a quantitative description of their ground-state structure evolution with deformation requires careful treatment of the pairing correlation. The Gogny-D1S pairing force is one of the best pairing forces for the study of nuclear structure. All these facts may also justify the use of the QCRHB-NL3 + separable Gogny D1S force theory to study the ground-state properties of the three nuclei. Certainly, as was mentioned at the end of the previous section, we have not yet performed the angular momentum projection in the QCRHB-NL3 + separable Gogny D1S force theory.

All the above comparisons allow us to draw the following conclusions: (a) the QCHFB full Gogny D1S approach is not so suited to study the ground-state PESs of the three nuclei; (b) the QCRHB-NL3 + separable Gogny D1S force theory has a good mean field and a pairing force, but it serves as only an approximation to the description of the ground-state PESs because it contains no angular momentum projection; and (c) the AMP-QCPC-PK1+BCS approach gives exact angular momentum projected PESs, but the underlying mean field and pairing force are less competitive than those used in the QCRHB-NL3 + separable Gogny D1S force theory.

The fact that the QCRHB-NL3 + separable Gogny D1S force theory yields results that are consistent with the experimental data, and its accuracy is as good as if not better than that of the AMP-QCPC-PK1+BCS approach, allows us to conclude that the QCRHB-NL3 + separable Gogny D1S force theory is a rather good approximation for the ground-state PES calculations of $^{80,82,84}$Zr nuclei. We note that the separation of the pairing interaction in this method reduces the computation time substantially. We hope that the angular momentum projection brings the results closer to the data.

### C. Shape coexistence

The coexistence of multiple shapes was first revealed in the proton-rich nuclei with $N = Z$ and $A = 72$–$92$ by Patra *et al.* based on an RMF approach [16]. Other theoretical results [68,69] support the existence of shape coexistence in zirconium isotopes. Experiments also showed the evidence of shape coexistence in nuclei of $^{82}$Zr and $^{84}$Zr [18,19]. In each of the $^{80,82,84}$Zr nuclei, multiple shapes can be seen, and two shapes coexist as shown in Fig. 1 where the ground-state PESs are calculated with the QCRHB-NL3 + separable Gogny D1S force theory. The reason for this is that the high-$j$ $g_{9/2}$ orbitals intrude into the $pf$ shell near the Fermi level as the deformation develops. The intrusion of the high-$j$ orbitals is also responsible for a pronounced shell effect at the superdeformations in $^{82}$Zr and $^{84}$Zr. For the three nuclei of $^{80,82,84}$Zr, although they have very similar occupied proton orbitals, their occupied neutron orbitals differ significantly. This difference results in the rapid change in their equilibrium shapes and the patterns of their shape coexistence. The PESs with the AMP-QCPC-PK1+BCS approach indicate that there is not any shape coexistence for $^{80}$Zr nucleus; however, shape coexistence occurs in $^{82,84}$Zr nuclei, which is different from that appearing in the PESs generated by the QCRHB-NL3 + separable Gogny D1S force theory, especially for the $^{82}$Zr nucleus (see Fig. 2). From Fig. 2 one can see clearly that the PESs obtained by the QCHFB full Gogny D1S approach show no shape coexistence phenomenon for any of the three nuclei. Therefore, the choice of the mean field and pairing interaction is rather crucial for the occurrence of the shape coexistence phenomenon in the three nuclei. The QCHFB full Gogny D1S approach fails to describe the equilibrium shapes and shape coexistence of the three nuclei.

### D. AMPPESs, shape transitions, and decay out of the SD bands

To study the shape evolution as spin increases, we calculated the AMPPESs with various angular momenta ($I = 0, 2, \ldots$) for $^{80}$Zr, $^{82}$Zr, and $^{84}$Zr by combining the QCRHB-NL3 + separable Gogny D1S force theory with the PSM (the description of this method can be found at the end of Sec. II). The results are shown in Fig. 3. One can see in Fig. 3 a pronounced SD rotational band in each of the three nuclei and a less pronounced vibrational-like ND band in $^{82}$Zr only. The assignment of the three SD rotational bands (vibrational-like ND band) is based on a fit of the energy versus spin sequences assuming a parabolic (linear) dependence. The features of the bands built on the spherical minima are different from nucleus to nucleus. The spherical band is an irregular (a single-particle)

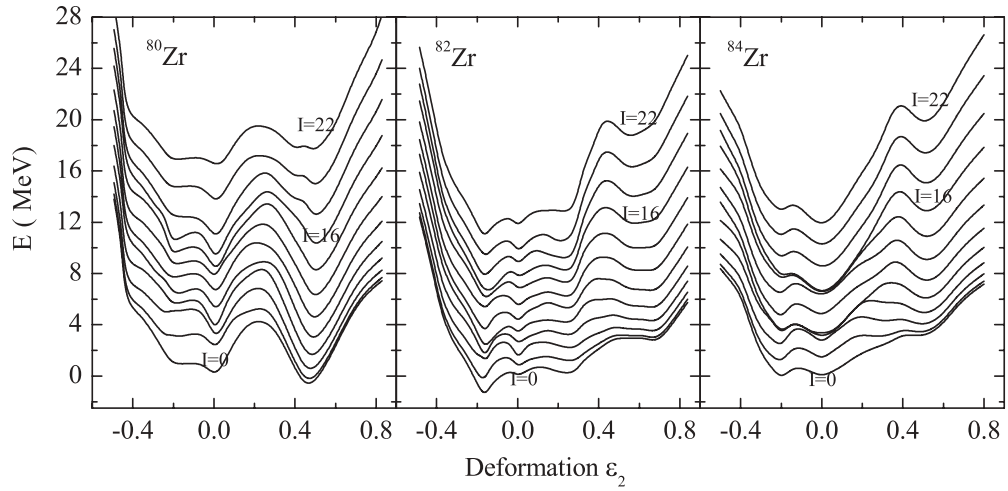


FIG. 3. Angular momentum projected potential energy surfaces for various spins as functions of deformation variable $\varepsilon_2$ for nuclei of $^{80}$Zr, $^{82}$Zr, and $^{84}$Zr, which are generated by combining the PSM with the QCRHB-NL3 + separable Gogny D1S force theory. The zero energy is set to be the ground-state total energy at $\varepsilon_2 = 0$.

excitation spectrum in $^{80}$Zr, and a vibrational-like band in both $^{82}$Zr and $^{84}$Zr. The vibrational-like bands might stem from the oscillation of the excess neutrons against the core ($^{80}$Zr). More excess neutrons benefit the collectivity of a nucleus and strengthen the oscillation. That might be the reason why the level spacing of the vibrational-like spectrum in $^{84}$Zr is large compared to that in $^{82}$Zr, and $^{84}$Zr is not as soft as $^{82}$Zr. Certainly, more excess neutrons complicate the oscillation. As a result, some spherical states of $^{84}$Zr are not vibrational-like ones. When the double semimagic nucleus of $^{80}$Zr remains spherical, its angular momentum comes mainly from the alignment of paired nucleons; therefore, its spherical band is dominated by a single-particle excitation spectrum. The bands built on the oblate minima also appear in these nuclei. The oblate band has a vibrational-like structure in $^{80}$Zr and $^{84}$Zr and a single-particle excitation feature in $^{82}$Zr.

With the AMPPESs and the nature of the bands discussed above, one can understand the phase-shape transitions and high spin structures of the three nuclei. A strong competition between different shapes is observed in these nuclei as spin increases. For instance, there is a prolate-spherical-oblate shape competition for the nucleus of $^{80}$Zr, especially at high spins. As a result, a phase-shape transition from prolate to spherical occurs at spin $I \approx 14$ as is shown in Fig. 3. A similar situation can be found for $^{84}$Zr, however; the shape transition is from oblate to spherical at spin $I \approx 12$. The above-mentioned two shape transitions are induced by spin, but they nevertheless stem from their ground-state shape coexistences; namely, the shape coexistences appear in the spin-zero potential energy surfaces (see Fig. 1). From Fig. 3, a strong oblate-spherical-prolate shape mixing can be observed in $^{82}$Zr, which is unique to this nucleus. The reason for this phenomenon might be that with adding two neutrons to the double semimagic nucleus $^{80}$Zr the competition between the single-particle motion and the collective motion becomes severe, and the nucleus changes its shape easily (it is rather soft), which leads to a strong competition among the oblate, spherical, and prolate shapes (see Fig. 1). Meanwhile, because of the oscillation of the excess neutrons against the core ($^{80}$Zr), the vibrational-like states dominate the excited spectra in a quite wide deformation range. Then it is difficult for the $^{82}$Zr nucleus to organize a collective rotation, and therefore no rotational band can be found in a wide deformation range, as shown in Fig. 3. Experimental data clearly show that the first rotational alignment begins at $I = 12$ for $^{82}$Zr [18], $I = 10$ for $^{84}$Zr [19], and a higher spin for $^{80}$Zr [50]. Therefore, it is understood that the rotation alignments induce the shape transitions in $^{80,84}$Zr nuclei. Note that almost all the calculated bands in the mass region of $N = Z$ and $A \approx 80$ show pronounced shape changes at rotational frequencies corresponding to the alignments of nucleons occupying states originating from $\pi g_{9/2}$ and $\nu g_{9/2}$ subshells. Satisfactory agreement between theory and experiment in the $T_z = 1$ nuclei analyzed in Ref. [18] as well as in the $T_z = 1/2$ nuclei $^{75}$Rb and $^{77}$Sr analyzed in Ref. [70] supports this scenario.

Another important feature should be pointed out that for nuclei $^{82}$Zr and $^{84}$Zr a superdeformation ($\varepsilon_2 \approx 0.55$) becomes more pronounced, namely, the minimum at the superdeformation gets deeper as spin increases, which can be clearly seen in Fig. 3. In 1995, Baktash *et al.* [6] provided the first evidence for the existence of a new region of high-spin superdeformation ($\beta_2 \approx 0.55$) in medium-mass nuclei from Sr to Zr isotopes with particle numbers $N, Z \approx 40$. Since then, a great deal of experimental work [7–9] about superdeformation was carried out in the $A = 80$ mass region. Among the three zirconium isotopes, only the SD bands in $^{84}$Zr have been observed so far. Recently, Chiara *et al.* [9] observed the decay-out of the SD band in $^{84}$Zr, which is rather fragmented. This is the first observation of such linking transitions in the $A \approx 80$ mass region.

One can see in Fig. 3 that for the $^{80}$Zr nucleus the barrier separating the SD and spherical states is high and thick for all spin values. Hence, the tunneling of the SD states into the spherical states through the barrier could be negligible;

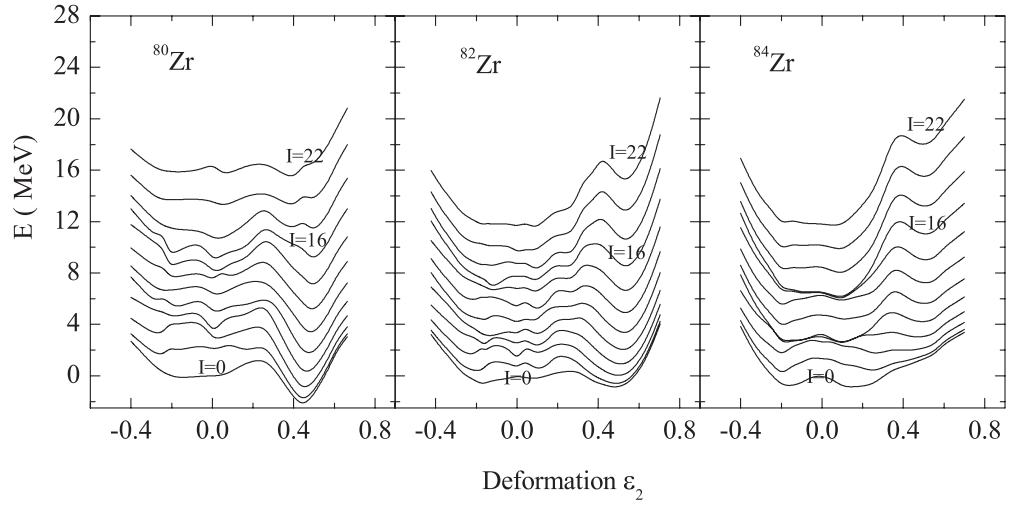


FIG. 4. Same as Fig. 3 but the angular momentum projected potential energy surfaces are obtained by combining the PSM with the AMP-QCPC-PK1+BCS approach.

namely, there is no decay out of the SD band in that nucleus. However, Fig. 3 shows that the barrier becomes lower and narrower for $^{82}$Zr and $^{84}$Zr nuclei at high spins. This implies that the decay out of the SD bands could occur at high spins for the two nuclei. Note that in Ref. [9] a study of least-action tunneling paths indicates that for the $^{84}$Zr nucleus the barrier separating the SD and ND states is very small. The decay out is actually attributed to a mixing of the SD states with the ND (or spherical) states with equal spin, which are close in energy to the SD states (more precisely, with the excited compound states which are located several MeV above the yrast ND states [71–74]). Because the typical energy difference between the SD states and ND (spherical) states is as high as 6–8 MeV for $^{82}$Zr and $^{84}$Zr nuclei at high spins, the decay-out intensity should be rather fragmented, as those found in $A = 150$ and 190 mass regions [75–79].

The AMPPESs discussed above are not exactly angular momentum projected, as we explained at the end of Sec. II. We used the same procedure described in Sec. II to recalculate the AMPPESs for $^{80,82,84}$Zr nuclei by combining the PSM with the AMP-QCPC-PK1+BCS approach instead of the QCRHB-NL3 + separable Gogny D1S force theory. The new AMPPESs are truly angular momentum projected because the ground-state PESs computed with the AMP-QCPC-PK1+BCS approach were angular momentum projected. The new AMPPESs for the three nuclei are presented in Fig. 4. Although the AMP-QCPC-PK1+BCS approach yields the equilibrium shapes for all three nuclei, which is consistent with the experimental data and predicts the shape coexistence in $^{82,84}$Zr nuclei, both the equilibrium shapes and shape coexistence differ significantly from those given by the QCRHB-NL3 + separable Gogny D1S force theory. The difference between the two kinds of ground-state PESs spreads out over the two kinds of AMPPESs as displayed in Figs. 3 and 4, which makes the two kinds of AMPPESs look different, especially at low spins. Nevertheless, from the new AMPPESs, one can find that there also exist shape transitions in $^{80,84}$Zr nuclei, which are less pronounced than those appearing in the old AMPPESs. Surprisingly enough, the two seemingly different kinds of AMPPESs share a few common aspects: (1)the strong oblate-spherical-prolate shape mixing exists in $^{82}$Zr; (2) the barrier separating the SD states and ND (spherical) states becomes lower and narrower for $^{82}$Zr and $^{84}$Zr nuclei at high spins, implying that the decay out of the SD bands could occur at high spins for the two nuclei; and (3) for nucleus $^{80}$Zr, the barrier is high and thick at all spin values, and there is no decay out of the SD band in that nucleus. Therefore, for the three nuclei, it seems that the strong shape mixing and decay out of the SD bands are not so sensitive to the choice of the bandheads (ground-state PESs).

## IV. SUMMARY

In this article, we investigated in detail the nuclear structure of the three proton-rich $^{80,82,84}$Zr nuclei. We calculated the ground-state PESs for these nuclei based on the QCRHB-NL3 + separable Gogny D1S force theory and compared them with those obtained with the AMP-QCPC-PK1+BCS approach and the QCHFB full Gogny D1S approach. It was shown that the QCRHB-NL3 + separable Gogny D1S force theory is a rather good approximation for the ground-state properties of these nuclei, although angular momentum projection was not included in this theory. This is probably because of the well-behaved mean field and pairing force used in this theory. The deformation values at the equilibrium shapes were determined by the ground-state PESs. The deformation values given by the QCRHB-NL3 + separable Gogny D1S force theory are different from those given by the AMP-QCPC-PK1+BCS approach, although both of them are consistent with the experimental data. The SPLs of these nuclei calculated with the QCRHB-NL3 + separable Gogny D1S force theory were used to understand their equilibrium shapes and shape coexistence. It was found that the minima of the total energies corresponded very well to the shell gaps of the single-particle levels. Based on the QCRHB-NL3 + separable Gogny D1S

force theory, we also found that, in each of the $^{80,82,84}$Zr nuclei, multiple shapes exist and two shapes coexist. The intrusion of the high-$j$ orbitals is responsible for this presence and for a pronounced shell effect at the superdeformations in $^{82}$Zr and $^{84}$Zr. For the three nuclei $^{80,82,84}$Zr, their occupied neutron orbitals differ significantly, which results in the rapid change in their equilibrium shapes and the patterns of their shape coexistence. Although the AMP-QCPC-PK1+BCS approach predicts the shape coexistence in $^{82,84}$Zr nuclei, this shape coexistence differs significantly from those given by the QCRHB-NL3 + separable Gogny D1S force theory.

Meanwhile, a method to calculate the AMPPESs was proposed for the first time that combines the projected shell model with the QCRHB-NL3 + separable Gogny D1S force theory. The AMPPESs calculations were carried out up to high spins for $^{80,82,84}$Zr nuclei. It was shown that shape transitions occur in $^{80}$Zr and $^{84}$Zr nuclei, which are driven by the rotational alignments of the nucleons in the $1g_{9/2}$ orbitals, and a strong shape mixing happens in $^{82}$Zr, which might originate from the competition between the single-particle motion and the collective motion. Moreover, we found that the barrier separating the SD states and ND (spherical) states becomes lower and narrower for nuclei $^{82}$Zr and $^{84}$Zr at high spins, which indicates that the decay out of the SD bands could occur at high spins for the two nuclei. The decay out could be rather fragmented since the energy difference between the SD states and ND (spherical) states is as high as 6–8 MeV for $^{82}$Zr and $^{84}$Zr nuclei at high spins. Nevertheless, for the $^{80}$Zr nucleus, there is no decay out of the SD band because the barrier is so thick. We hope future experiments would confirm our prediction. We recalculated the AMPPESs of $^{80,82,84}$Zr nuclei by replacing the QCRHB-NL3 + separable Gogny D1S force theory by the AMP-QCPC-PK1+BCS approach, and we found that the two kinds of AMPPESs have a few common features: the strong shape mixing in $^{82}$Zr and the decay out of the SD bands in $^{82,84}$Zr nuclei, although at low spins they are different from each other. The common features imply that the strong shape mixing and the decay out of the SD bands are not so sensitive to the choice of the bandheads.

## ACKNOWLEDGMENTS

We are grateful to Professor Xi-Zhen Zhang for very helpful discussions. This work was supported in part by the National Natural Science Foundation of China under Grants No. 10675170 and No. 10975190 and the Major State Basic Research Developing Program under Grant No. 2007CB815003.

[1] J. H. Hamilton *et al.*, Phys. Rev. Lett. **32**, 239 (1974).
[2] C. Chandler *et al.*, Phys. Rev. C **56**, R2924 (1997).
[3] F. Becker *et al.*, Eur. Phys. J. A **4**, 103 (1999).
[4] E. Bouchez *et al.*, Phys. Rev. Lett. **90**, 082502 (2003).
[5] W. Korten *et al.*, Nucl. Phys. A **752**, 255C (2005).
[6] C. Baktash *et al.*, Phys. Rev. Lett. **74**, 1946 (1995).
[7] H.-Q. Jin *et al.*, Phys. Rev. Lett. **75**, 1471 (1995).
[8] F. Lerma *et al.*, Phys. Rev. Lett. **83**, 5447 (1999).
[9] C. J. Chiara *et al.*, Phys. Rev. C **73**, 021301(R) (2006).
[10] F. Dickmann, V. Metag, and R. Repnow, Phys. Lett. B **38**, 207 (1972).
[11] W. Nazarewicz *et al.*, Nucl. Phys. A **435**, 397 (1985).
[12] P. Bonche *et al.*, Nucl. Phys. A **443**, 39 (1985).
[13] M. Girod, J. P. Delaroche, D. Gogny, and J. F. Berger, Phys. Rev. Lett. **62**, 2452 (1989).
[14] G. A. Lalazissis and M. M. Sharma, Nucl. Phys. A **586**, 201 (1995).
[15] G. A. Lalazissis, S. Raman, and P. Ring, At. Data Nucl. Data Tables **71**, 1 (1999).
[16] S. K. Patra, B. K. Raj, M. S. Metha, and R. K. Gupta, Phys. Rev. C **65**, 054323 (2002).
[17] M. Bender, G. F. Bertsch, and P. H. Heenen, Phys. Rev. C **73**, 034322 (2006).
[18] D. Rudolph *et al.*, Phys. Rev. C **56**, 98 (1997).
[19] R. Cardona *et al.*, Phys. Rev. C **68**, 024303 (2003).
[20] D. Vretenar, A. V. Afanasjevb, G. A. Lalazissis, and P. Ring, Phys. Rep. **409**, 101 (2005).
[21] G. A. Lalazissis, J. König, and P. Ring, Phys. Rev. C **55**, 540 (1997).
[22] Y. Tian, Z. Y. Ma, and P. Ring, Phys. Lett. B **676**, 44 (2009).
[23] J. F. Berger, M. Girod, and D. Gogny, Nucl. Phys. A **428**, 32C (1984).
[24] I. Talmi, Helv. Phys. Acta **25**, 185 (1952).
[25] M. Moshinsky, Nucl. Phys. **13**, 104 (1959).
[26] T. A. Brody, G. Jacob, and M. Moshinsky, Nucl. Phys. **17**, 16 (1960).
[27] K. Hara and Y. Sun, Int. J. Mod. Phys. E **4**, 637 (1995).
[28] Y. Sun and J. A. Sheikh, Phys. Rev. C **64**, 031302(R) (2001).
[29] R. Palit, J. A. Skeikh, Y. Sun, and H. C. Jain, Nucl. Phys. A **686**, 141 (2001).
[30] S. G. Nilsson *et al.*, Nucl. Phys. A **131**, 1 (1969).
[31] S. Shen *et al.*, Phys. Lett. B **554**, 115 (2003).
[32] G. Audi *et al.*, Nucl. Phys. A **729**, 337 (2003).
[33] P. Möller *et al.*, At. Data Nucl. Data Tables **59**, 185 (1995).
[34] Y. Sun, J. Zhang, M. Guidry, J. Meng, and S. Im, Phys. Rev. C **62**, 021601(R) (2000).
[35] T. Bengtsson and I. Ragnarsson, Nucl. Phys. A **436**, 14 (1985).
[36] Y. Sun and K. Hara, Comput. Phys. Commun. **104**, 245 (1997).
[37] H. Kucharek and P. Ring, Z. Phys. A **339**, 23 (1991).
[38] P. Ring, Prog. Part. Nucl. Phys. **37**, 193 (1996).
[39] G. A. Lalazissis, D. Vretenar, and P. Ring, Phys. Rev. C **57**, 2294 (1998).
[40] G. A. Lalazissis, D. Vretenar, P. Ring, M. Stoitsov, and L. Robledo, Phys. Rev. C **60**, 014310 (1999).
[41] G. Lalazissis, D. Vretenar, and P. Ring, Nucl. Phys. A **650**, 133 (1999).
[42] T. Duguet, Phys. Rev. C **69**, 054317 (2004).
[43] Y. Tian and Z. Y. Ma, Chin. Phys. Lett. **23**, 3226 (2006).
[44] J. Dechargé and D. Gogny, Phys. Rev. C **21**, 1568 (1980).
[45] J. F. Berger, M. Girod, and D. Gogny, Comput. Phys. Commun. **63**, 365 (1991).
[46] Y. Tian, Z. Y. Ma, and P. Ring, Phys. Rev. C **80**, 024313 (2009).
[47] P. Ring, Y. K. Gambhir, and G. A. Lalazissis, Comput. Phys. Commun. **105**, 77 (1997).

[48] A. Bohr and B. R. Mottelson, *Nuclear Structure* (World Scientific, Singapore, 1998), Vol. 2: Nuclear deformations.
[49] P. Ring and P. Schuck, *The Nuclear Many Body Problem* (Springer-Verlag, New York, 1980).
[50] S. M. Fischer *et al.*, Phys. Rev. Lett. **87**, 132501 (2001).
[51] S. Hilaire and M. Girod, Eur. Phys. J. A **33**, 237 (2007).
[52] [http://www-phynu.cea.fr/HFB-Gogny_eng.htm].
[53] A. Valor, P. H. Heenen, and P. Bonche, Nucl. Phys. A **671**, 145 (2000).
[54] M. Bender, P. H. Heenen, and P. G. Reinhard, Rev. Mod. Phys. **75**, 121 (2003).
[55] M. Bender, G. F. Bertsch, and P. H. Heenen, Phys. Rev. C **73**, 034322 (2006).
[56] M. Bender, P. Bonche, and P. H. Heenen, Phys. Rev. C **74**, 024312 (2006).
[57] R. Rodríguez-Guzmán, J. L. Egido, and L. M. Robledo, Phys. Rev. C **65**, 024304 (2002).
[58] R. Rodríguez-Guzmán, J. L. Egido, and L. M. Robledo, Nucl. Phys. A **709**, 201 (2002).
[59] T. Nikšić, D. Vretenar, and P. Ring, Phys. Rev. C **73**, 034308 (2006).
[60] T. Nikšić, D. Vretenar, and P. Ring, Phys. Rev. C **74**, 064309 (2006).
[61] J. M. Yao, J. Meng, P. Ring, and D. Pena Arteaga, Phys. Rev. C **79**, 044312 (2009).
[62] B. A. Nikolaus, T. Hoch, and D. G. Madland, Phys. Rev. C **46**, 1757 (1992).
[63] T. Bürvenich, D. G. Madland, J. A. Maruhn, and P. G. Reinhard, Phys. Rev. C **65**, 044308 (2002).
[64] J. L. Friar, D. G. Madland, and B. W. Lynn, Phys. Rev. C **53**, 3085 (1996).
[65] P. W. Zhao *et al.*, arXiv:1002.1789v1 [nucl-th].
[66] G. A. Lalazissis, S. Raman, and P. Ring, At. Data Nucl. Data Tables **71**, 1 (1999).
[67] T. Gonzales-Llarena *et al.*, Phys. Lett. B **379**, 13 (1996).
[68] M. Yamagami, K. Matsuyanagi, and M. Matsuo, Nucl. Phys. A **693**, 579 (2001).
[69] A. Petrovici, K. W. Schmid, and A. Faessler, Nucl. Phys. A **708**, 190 (2002).
[70] C. J. Gross *et al.*, Phys. Rev. C **56**, R591 (1997).
[71] E. Vigezzi, R. A. Broglia, and T. Døssing, Nucl. Phys. A **520**, 179C (1990).
[72] J. Z. Gu and H. A. Weidenmüller, Nucl. Phys. A **660**, 197 (1999).
[73] H. A. Weidenmüller and G. E. Mitchell, Rev. Mod. Phys. **81**, 539 (2009).
[74] J. Z. Gu *et al.*, Nucl. Phys. A **834**, 87C (2010).
[75] P. J. Twin *et al.*, Phys. Rev. Lett. **57**, 811 (1986).
[76] T. L. Khoo *et al.*, Phys. Rev. Lett. **76**, 1583 (1996).
[77] A. Dewald *et al.*, Phys. Rev. C **64**, 054309 (2001).
[78] A. N. Wilson, Prog. Theor. Phys. Suppl. **154**, 138 (2004).
[79] A. N. Wilson, A. J. Sargeant, P. M. Davidson, and M. S. Hussein, Phys. Rev. C **71**, 034319 (2005).